SIMULATION OF ROUGH-WALL TURBULENT BOUNDARY LAYER FOR LES INFLOW DATA

Kojiro Nozawa
Izumi Research Institute, Shimizu Corp.
2-2-2 Uchisaiwai-cho, Chiyoda-ku, Tokyo 100-0011, Japan
nozawa@ori.shimz.co.jp

Tetsuro Tamura
Dept. of Environmental Science and Technology, Tokyo Institute of Technology
4259 Nagatsuta, Midori-ku, Yokohama 226-8502, Japan
tamura@depe.titech.ac.jp

ABSTRACT

A method of generating rough-wall turbulent LES inflow data using periodic boundary condition is proposed. The rough surface is realized by rectangular blocks arrayed on the surface. The rough-wall turbulent boundary layers are simulated using the proposed method. The Reynolds number based on momentum thickness and the free stream is about 13,000 in the simulations. The mean velocity profile is in good agreement with the slope of u_τ/κ and the values of velocity fluctuations are in the range of various experimental data. The influence of using periodic boundary conditions on the characteristics of turbulence is revealed by comparing the results whose length of periodic regions are different.

INTRODUCTION

In many engineering fields, obstacles are immersed in turbulent boundary layers developing over hydrodynamically rough surfaces. In order to simulate the flow around the obstacles numerically, time-dependent turbulent inflow conditions are required at the upstream boundary. The method of inflow generation which accounts for spatial growth in periodic domains was proposed by Spalart and Leonard (1985), and then modified by Lund *et al.* (1998) who applied the method to a Cartesian coordinate system and therefore added rescaling parameters. These methods are originally limited to the generation of turbulent boundary layer over smooth surfaces. In order to apply the methods to the rough-wall turbulent boundary layer, the modification of the periodic boundary conditions and the surface boundary conditions are required. In this paper the method of Lund is modified to simulate a turbulent boundary layer develops over rough-wall. The empirical resistance formula of sand-roughened plate is introduced to determine the rescaling parameters of the periodic boundary conditions. Rectangular blocks are arrayed on the surface to realize the rough surface with slightly increasing the CPU cost. Turbulent boundary layers developing over rough surfaces are simulated using the proposed method and the results are compared with the results of a simulation of a turbulent boundary layer developing over smooth surface. The influence of using the periodic boundary conditions on the characteristics of turbulent boundary layer is also studied.

GENERATION OF TURBULENT BOUNDARY LAYER

The idea of Lund's method is to estimate the velocity at the inlet plane based on the solution downstream and apply outflow boundary conditions at the exit boundary (see Fig.1). The flow is assumed to have self-similarity in vertical direction. The velocity of downstream station is rescaled and reintroduced to the inlet. The mean flow is rescaled due to the "law of the wall" in the inner region and "defect law" in the outer region.

The rescaling procedure in both the inner and the outer region can be written as

$$\begin{cases} U_{inlt} &= \gamma U_{recy}(z^*_{inlt}) \\ u'_{inlt} &= \gamma u'_{recy}(z^*_{inlt}) \\ u_{inlt} &= U_{inlt} + u'_{inlt} \end{cases}$$

and

$$\begin{cases} (U_\infty - U)_{inlt} &= \gamma(U_\infty - U)_{recy}(\eta_{inlt}) \\ u'_{inlt} &= \gamma u'_{recy}(\eta_{inlt}) \\ u_{inlt} &= U_{inlt} + u'_{inlt}, \end{cases}$$

where,$z^* = z/l_{inn}$ is the inner coordinate (l_{inn} is the length scale for inner region), $\eta = z/l_{out}$ is the outer coordinate (l_{out} is the length scale for outer region), $\gamma = \frac{u_{\tau(inlt)}}{u_{\tau(recy)}}$ is the ratio of the friction velocity.

The parameters in this rescaling procedure are γ and $\beta(= \frac{\theta_{inlt}}{\theta_{recy}})$, which is the ratio of the momentum thickness at the inlet to that at the recycle station. Both β and γ are not independent parameter and γ is determined by β using the Blasius's pipe resistance formula theory. The formula is limited to the flow over smooth surface, we have to introduce a new relation between β and γ to apply this method to the flow over rough surface.

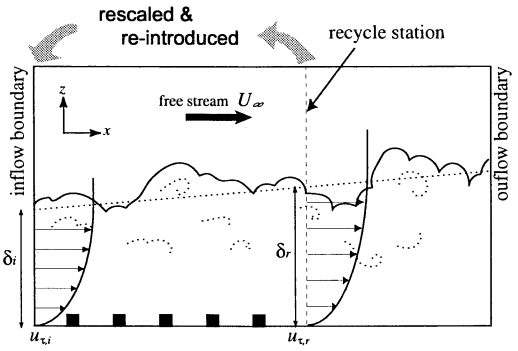

Figure 1: Schematic presentation of Lund's method with roughness blocks.

Modification of Lund's method

We apply the resistance formula of sand-roughened plate by Prandtl (Sclichting, 1979) to determine rescaling parameter γ from β. The interpolation formulae for the coefficients of skin friction in terms of relative roughness can be written as follow

$$c'_f(x) = \left(2.87 + 1.58 \log \frac{x}{k_s}\right)^{-2.5}, \quad (1)$$

where k_s is equivalent sand roughness, x is the estimated distance from the leading edge. With the assumption of linear interpolation on a log scale, equation (1) can be lead to

$$\frac{c'_f(x)}{c'_f(x_a)} = \left(\frac{x}{x_a}\right)^{-r},$$

where,

$$r = \frac{3.95}{2.87 + 1.58 \log \frac{x}{k_s}}.$$

By integrating the equation from 0 to x, the relation between γ and β could be derived as follows.

$$\beta^{-1} - 1 = \frac{c'_f(x)}{2\theta_{inlt}} \frac{x}{1-r} \left\{\gamma^{\frac{2r-2}{r}} - 1\right\}$$

In the above relation, rescaling parameter β could be determined from the mean velocity profile at the recycle station and the unknown parameter is the estimated distance x. The distance x could be estimated from the von Kármán's momentum-integral equation and another resistance formula of sand-roughened plate, which is for total skin friction. The definition of the total skin friction $C_f(x)$ is

$$C_f(x) \equiv \frac{D(x)}{(1/2)\rho U_\infty^2 bx}.$$

The total drag force $D(x)$ can be written as

$$\begin{aligned} D(x) &= \rho U_\infty^2 \int_0^x d\theta \\ &= \rho U_\infty^2 \theta(x), \end{aligned}$$

and the relation between $C_f(x)$ and θ can be derived as

$$C_f(x) = \frac{2\theta(x)}{2}.$$

The formula of Prandtl's total skin friction is as follow.

$$C_f(x) = \left\{1.89 + 1.62 \log \frac{x}{k_s}\right\}^{-2.5}$$

From the two equation, we can get the equation as

$$\theta^* = \frac{x^*}{2} (1.89 + 1.62 \log x^*)^{-2.5},$$

where $\theta^* = \theta/k_s$, $x^* = x/k_s$.

The momentum thickness at the recycle station θ can be determined from the mean velocity profile, while θ_{inlt} can be given in controlling the momentum thickness. The distance from the leading edge x was derived using iteration method to the above equation. In this simulation, any formulation of mean velocity profile is not given to the procedure.

NUMERICAL METHOD

In order to validate the proposed method, a rough-wall turbulent boundary layer was simulated. The Navier-Stokes equations for an incompressible fluid combined with subgrid-scale viscosity are used for the large eddy simulation (LES). Smagorinsky model with Van-Driest type damping function is used in this simulation, because of the simple geometric computational domain. The whole computational domain is divided into three with horizontal section to change the grids resolution in horizontal direction. In the near wall region, the mesh resolution was not fine enough to resolve the organized turbulence structures, such as low- and high-speed streaks.

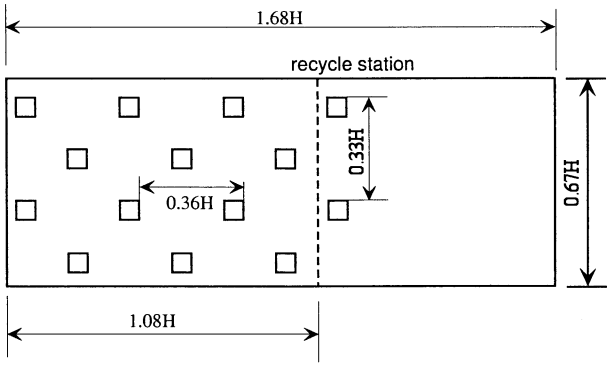

Figure 2: Computational domain and the arrange of roughness blocks.

Table 1: Size and location of roughness block.

depth	h_x/H	0.040
width	h_y/H	0.030
height	h_z/H	0.030
mean separation distance	D	0.246
roughness density	λ	0.015
grid points	$n_x \times n_y$	6×8

Rectangular blocks, with the size $0.04H \times 0.03H \times 0.03H$ (H is the height of computational domain), are arrayed on the surface in a staggered location to realize the surface roughness. Several blocks are also located downstream of the recycle station to keep the periodicity. From the standpoint that the loss of bulk momentum must be the key factor, each blocks is covered with the zone where the simplified cubic interpolated pseudo-particle (CIP) method (Takewaki, 1985; Takiguchi, 1998) is applied to the convection terms of the Navier-Stokes equations. The zone covers just three grids outside the surface of the blocks. The top surface of a roughness block is expressed only by 6×8 grids with same spacing. By applying the CIP method, the increase of CPU cost in treating the rectangular blocks is small. The mean separation distance of the roughness D is about 0.25H, and the roughness concentration λ is about 0.015 in this simulation. A momentum thickness Reynolds number was $R_\theta = 13,000$.

RESULTS

Figure 3 shows instantaneous isosurface of second-invariants of deformation tensor near the surface. Complicated vortical structures could be seen formed in the wake of roughness blocks.

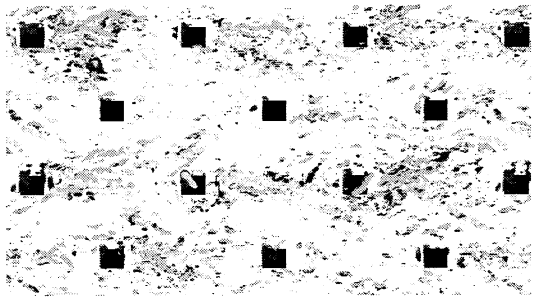

Figure 3: Instantaneous vortical structures in the wake of roughness blocks(isosurface of second-invariants of deformation tensor).

mean profiles

Mean velocity profiles are shown in Fig.4. In order to compare with the result of the rough-wall boundary layer simulation, the result of a smooth-wall boundary layer simulation using the original Lund's method is also shown in the figure. The height z and the displaced height $(z-d)$ are normalized using the boundary thickness δ. In the logarithmic region, the mean velocity profile of the rough-wall boundary layer simulation is in good agreement with the slope of u_τ/κ (dotted lines in the figures), where κ is the Kármán constant and u_τ is the friction velocity estimated from the peak value of Reynolds stress. The zero-plane displacement d evaluated by the mean profile is $0.015H$ and it corresponds with that evaluated by the vertical profile of Reynolds stress $\overline{u'w'}$ using the theory that d is the mean height of momentum absorption (Thom, 1971 and Jackson, 1981). A roughness length z_0 is $0.0032H$ and the ratio z_0/h is 0.011 in the rough-wall simulation. The roughness density in this simulation is $\lambda = 0.015$ and it is almost as same as the ratio z_0/h which is considered to have a relation with the roughness density (Raupach, 1991).

The vertical profiles of velocity fluctuations are shown in Figure 5. It has been found that ratio σ_u/u_τ, σ_v/u_τ, σ_w/u_τ takes values

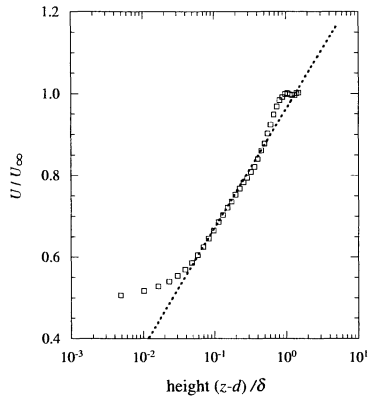

(a) rough wall

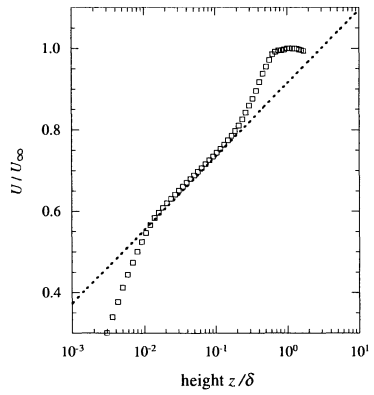

(b) smooth wall

Figure 4: Mean velocity profile.

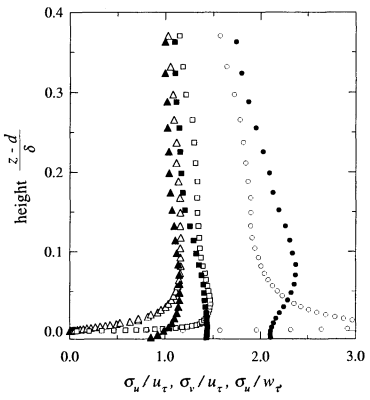

Figure 5: Profiles of turbulence velocity components: •, flow over rough-wall; ○, flow over smooth-wall.

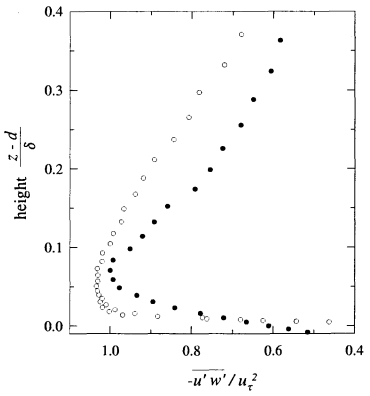

Figure 6: Profiles of turbulent shear stress: Symbols in Figure 5.

(at $\frac{z-d}{\delta} = 0.1$) of about 2.1 ± 0.2, 1.4 ± 0.1 and 1.1 ± 0.1 respectively (Raupach, 1991). Although the time averaging was not enough in both simulations, the values of the rough-wall simulation are in the range respectively. The profiles are almost similar in the outer region except the σ_u/u_τ. The values of σ_u/u_τ in the smooth-wall simulation are lower in the outer region and the peak value near the surface is much higher than that in the rough-wall simulation. The trend that the smooth wall data takes the higher peak values can be seen in various experiments.

The vertical profiles of Reynolds stress $\overline{u'w'}$ are shown in Figure 6. The values of $\overline{u'w'}$ in the rough-wall simulation are lower than those in the smooth-wall simulation. The same trend can be seen in the experimental data by Antonia and Luxton (1971). In the rough-wall simulation the values of $\overline{u'w'}$ decline slowly compared with those in smooth-wall simulation near the wall. This difference comes from the difference between the flat surface and the rough surface. In the rough-wall simulation the estimated displaced heigh is about one half of the height of a roughness block and the values of $\overline{u'w'}$ declines slowly and becomes zero at the surface.

Influence of periodic boundary condition

The influence of using periodic boundary conditions on the characteristics of turbulent boundary layer was studied by changing the length of the periodic region (the region is from the inlet plane to the recycle station; see Table 2). The length of the periodic region in the case B is double of that in the case A. Other computational conditions were same as the former simulation. Figure 7 shows power spectra of streamwise fluctuation velocities. k_x is the wavenumber in streamwise direction normalized by the length of grid spacing Δx. At high wavenumbers, the slopes of the spectra collapse to $-2/3$ power law and there are no difference between the two cases. At low wavenumbers, the local peaks in the case A can be seen in the lower wavenumbers than those in the case B (dotted vertical lines indicate the length of periodic boundary regions). The difference in the locations of the local peaks between the

Table 2: Computational region (streamwise direction).

	case A	case B
length of the periodic region	$1.08H$	$2.16H$
length of the comp. region	$1.68H$	$2.76H$

two cases appears in the higher region ($z/H > 0.065$). The sharp peaks appear in wavenumber about $k_x = 0.02$ are caused by the spacing of the arrayed roughness blocks.

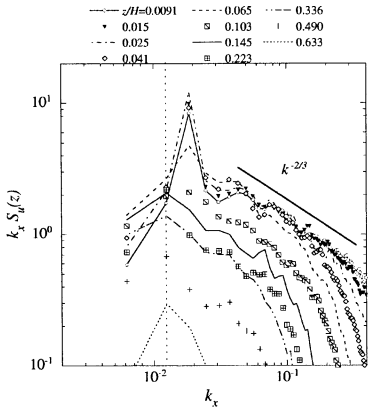

(1) ケース A

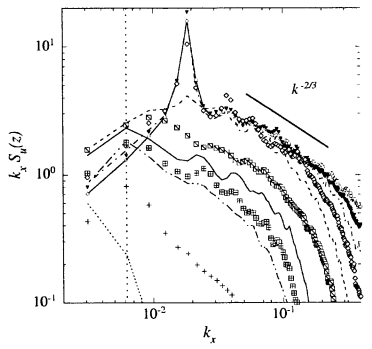

(2) ケース B

Figure 7: Spectrum of streamwise velocities (pre-multiplied spectra).

Figure 8 shows the integral scales of turbulence in streamwise direction. The integral scales L_u^x are estimated assuming that the ensemble average of cross-covariance functions fit with the exponential function ($f(r) = exp(-r/L_u^x)$; r is the distance). Although the integral scales in a turbulent boundary layer is considered to increase monotonously as the height increase, they begin to decline at the height $(z-d)/\delta = 0.06$ in the case A and 0.14 in the case B. The length of the coherent structure at $z = 0.10H$ is almost as same as the thickness of the turbulent boundary layer and it is almost same as the length of the periodic region in the case A(Figure 9). These results shows that in the case A the periodic region influences the size of coherent structure at the higher region($z/H > 0.065$) of the generated boundary layer. However, the influence of the periodic region could be decreased by extending the periodic region as seen in the case B.

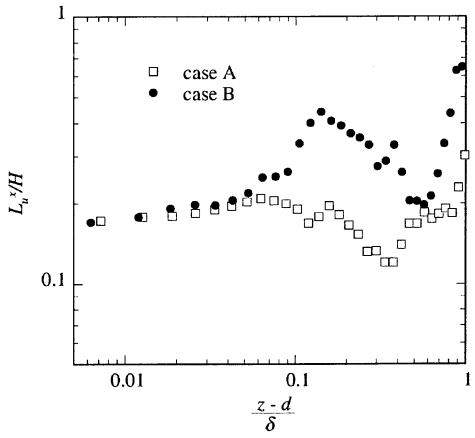

Figure 8: Integral scale of turbulence in streamwise direction (streamwise velocity).

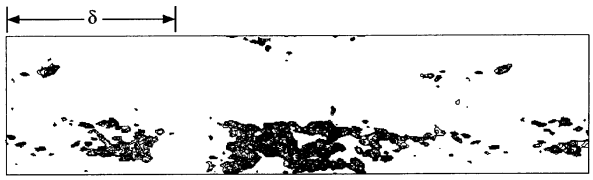

(a) $z = 0.10H$

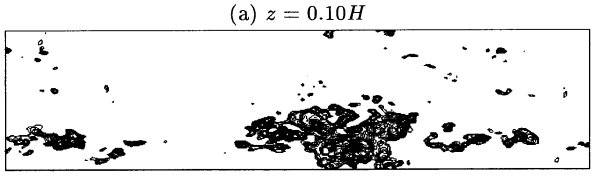

(b) $z = 0.22H$

Figure 9: Coherent structure in boundary flow in case B (darkened parts $u > U(z) + \frac{1}{2}\sigma_u$) .

SIMULATION AROUND A RECTANGULAR OBSTACLE USING GENERATED INFLOW DATA

The generated inflow data, the rough-wall inflow data and the smooth-wall inflow data, are applied to the simulations of flows around a rectangular obstacle. The smooth-wall turbulent inflow data were generated using the original Lund's method accompany with the rough-wall inflow data to clarify the difference of characteristic of incoming turbulence. The rectangular obstacle is half height cube and its height is about 0.17 of the boundary layer thickness of inflows. Figure 4 shows the mean flow patterns of the centerline of the obstacles. In the case of rough-wall turbulence, the size of a separation bubble organized over the top surface of the obstacle was smaller than

that in the case of smooth-wall turbulence. In the case of rough-wall the pressure on the top surface recovers faster than that in the case of smooth-wall. The difference in characteristics of flows around the obstacles comes from the difference in turbulent characteristics of approaching flows. The pressure distributions on the roof of the obstacles are almost similar to the experimental data respectively.

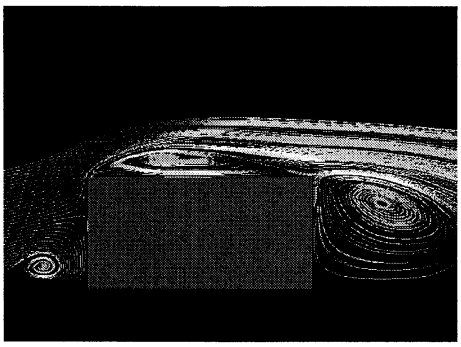

(a) smooth-wall

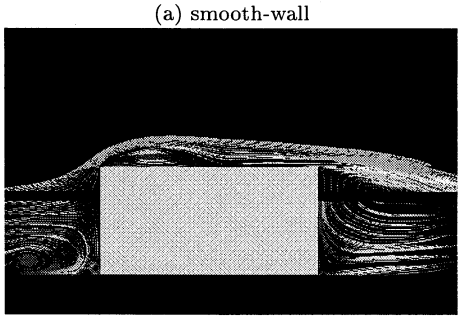

(b) rough-wall

Figure 10: Streamlines of the mean flow projected onto the centerline of the obstacle.

SUMMARY

The method of simulating rough-wall turbulent boundary layers for LES inflow data has been proposed. In order to realize the effects of a rough wall, rectangular blocks are arrayed on the surface in a staggered location. The mean streamwise velocity profile of the rough-wall boundary layer simulation using the proposed method was in good agreement with the slope of u_τ/κ. The ratio σ_u/u_τ, σ_v/u_τ, σ_w/u_τ at $(z-d)/\delta = 0.1$ were in the range of various experimental data.

The influence of using periodic boundary conditions in streamwise direction has been studied by changing the length of the periodic region. The influence was appeared in the integral scales of turbulence and the local peak of spectrum of streamwise fluctuation velocity. The integral scales of turbulence were underestimated in the higher region where the length of the coherent structures become longer than the length of periodic region. Although, the influence is limited to the higher region and could be decreased by extending the length of the periodic region.

The generated inflow data were applied to the simulations of flows around a rectangular obstacle. The mean flows around the obstacle were different between the two cases, which use the rough-wall inflow data and the smooth-wall inflow data.

References

Antonia, R. A. and Luxton, R. E., 1971, "The response of a turbulent boundary layer to a step change in surface roughness: Part 1. Smooth to rough", *J. Fluid Mech.*, Vol.48, part 4, pp.721-761.

Jackson, P. S., 1981, "On the displacement height in the logarithmic velocity profile", *J. Fluid Mech.*, Vol.111, pp.15–25.

Lund, T. S., Wu, X. and Squires, K. D., 1998, "Generation of Turbulent Inflow Data for Spatially-Developing Boundary Layer Simulations", *Journal of Computational Physics* **140**, pp.233–258.

Raupach, M. R., Antonia, R. A. and Rajagopalan, S., 1991, "Rough-wall turbulent boundary layers", *Appl. Mech. Rev,*, Vol.44, no.1, pp.1–25.

Schlichting, H., 1979, "Boundary-Layer Theory, 7th Edition", McGraw-Hill Book Company.

Spalart, P. R. and Leonard, A., 1987, "Direct numerical simulation of equilibrium turbulent boundary layers", In *Turbulent Shear Flows 5*, pp.235–252,

Takewaki, H, Nishiguchi, A. and Yabe, T., 1985, "Cubic interpolated pseudo-particle method (CIP) for solving hyperbolic-type equations", *J. Comp. Phys.*, Vol.61, pp.261-268.

Takiguchi, S., Kajishima, T. and Miyake, Y., 1998, "Numerical Scheme to Resolve the Interaction between Solid-Particles and Fluid-Turbulence", *Trans. of the Japan Society of Mech. Eng.***64**, no.625, pp.2804–2810 (*in Japanese*).

Thom, A. S., 1971, "Momentum absorption by vegetation", *Quart. J. Roy. Meteorol. Soc.*, No.97, pp.414–428.